Swansea University
School of the Environment & Society

Algorithm Theoretical Basis Document

PROBA/CHRIS
Aerosol Optical Depth Retrieval Module

Version 3.0, 7th April 2008

William Grey* and Peter North

School of the Environment and Society, Swansea University, Singleton Park, Swansea, SA2 8PP, UK.

*Email: w.m.f.grey@swan.ac.uk

**Development of PROBA/CHRIS Modules for the BEAM toolbox
(ESA ITT SoWENVI-DTEX-EOPS-SW-06-0008)**

Table of Contents

Acronyms and Abbreviations

ATBD	Algorithm Theoretical Basis Document
AATSR	Advanced Along-Track Scanning Radiometer
AERONET	AErosol RObotic NETwork
AOD	Aerosol Optical Depth
BAER	Bremen Aerosol Retrieval
BRDF	Bi-directional Reflectance Distribution Function
BEAM	Basic ERS and Envisat (A)ATSR and MERIS
CHRIS	Compact High Resolution Imaging Spectrometer
DEM	Digital Elevation Model
ESA	European Space Agency
fAPAR	Fraction of Absorbed Photosynthetically Active Radiation
GPOD	Grid-Processing On Demand
IDL	Interactive Data Language
LAI	Leaf Area Index
MODIS	MODerate Resolution Imaging Spectrometer
MODTRAN	MODerate spectral resolution atmospheric TRANSmittance algorithm
MISR	Multi-angle Imaging Scanning Radiometer
MERIS	MEdium Resolution Scanning Radiometer
NDVI	Normalised Difference Vegetation Index
NERC	Natural Environment Research Council
PROBA	PRoject for On-Board Autonomy
RMSE	Root Mean Square Error
RAA	Relative Azimuth Angle
SWIR	ShortWave InfraRed
SZA	Solar Zenith Angle
TOA	Top Of Atmosphere
VZA	View Zenith Angle

Abstract

We present an algorithm that retrieves atmospheric aerosol optical depth (AOD) over land using data acquired by the CHRIS (Compact High Resolution Imaging Spectrometer) instrument that is on-board the PROBA (Project for On-Board Autonomy) spaceborne platform. The algorithm exploits the multi-view-angle capability of CHRIS for AOD retrieval. Pre-calculated lookup tables of atmospheric properties for a given aerosol model allow fast retrievals over entire CHRIS scenes. We have developed a prototype AOD retrieval module for implementation within the BEAM (Basic Envisat AATSR and MERIS) toolbox that is both flexible and straightforward to use. Testing has been performed against a simulated dataset of TOA reflectances corresponding to the CHRIS instrument characteristics that are created from coupled surface and atmospheric radiative transfer model runs for a representative set of surface and atmospheric conditions. The RMSE between the forward modelled AOD and the retrieved AOD is less than 0.04. Validation of PROBA/CHRIS retrievals of AOD have also been carried out against AERONET derived AOD for 29 scenes at six sites worldwide. Across all sites the Pearson's correlation coefficient has been calculated to be 0.69 with a RMSE (root mean square error) of 0.11.

1. Introduction

1.1 Rationale

Atmospheric aerosols play a key role in the radiative forcing of the Earth's climate. Firstly, aerosols have a direct effect on the Earth's radiation budget by reflecting some of incoming solar energy back into space.   Secondly, aerosols indirectly affect the radiation budget through their influence on cloud properties and albedo. Globally, the net radiative forcing of aerosols is negative, thereby offsetting some of the potential warming caused by increasing atmospheric carbon concentrations.   Aerosols also influence other aspects of the climate system such as the biogeochemical and hydrological cycles. For instance, aerosols affect the total and diffuse radiation fraction at the surface which has consequences on carbon assimilation by vegetation. Moreover, large concentrations of aerosols are thought to lead to precipitation suppression, as is the case for dust in the West-African Sahel.

Yet aerosols remain a major source of uncertainty in our understanding of the climate system. Recently, there has been a concerted effort by the climate community to gain knowledge through long term monitoring stations, intensive field campaigns, development of models and Earth observations. The Compact High Resolution Imaging Spectrometer (CHRIS) is one spaceborne remote sensing instrument that can make an important contribution to this endeavour. CHRIS allows detailed spatial information on aerosols over local areas to be obtained and its high-level of specification allows for extensive experimentation which is useful for designing future missions.   Moreover, it will be useful for testing other satellite derived datasets of AOD.

1.2 CHRIS instrument characteristics

CHRIS was launched on-board the PROBA (Project of On-Board Autonomy) platform in October 2001 as an experimental mirco-satellite demonstration of new technologies (Barnsley *et al*., 2004). Originally designed as a 1-year mission it has far exceeded its planned life-time and will continue to acquire data for the foreseeable future. CHRIS acquires images at a high spatial resolution (17 or 34 meters) for up to 62 narrow bands in the optical region between 400 and 1050 nm. A novel characteristic of the PROBA platform is its maneuverability allowing CHRIS' single push-broom scanner to be pointed at a specified target up to five times during the acquisition of the multi-view-angle set of images. The viewing zenith

angles are nominally given as 55° and 36° in the backwards and forwards direction, and at nadir. All 5 CHRIS scenes are acquired within 7 minutes during an imaging sequence. A full width CHRIS scene at nadir typically covers a 13 by 13 km area. Owing to the limited on-board data storage, only a single multi-angle set of images can be acquired per orbit before the data are downloaded at the Kiruna ground receiving station in Sweden. In addition, the full capability of CHRIS cannot be realised for any given acquisition sequence. Instead, there are a range of modes of data that can be selected for specific applications as shown in Table 1.

Table 1: Characteristics of the PROBA/CHRIS modes (Sira, 2005).

Mode	Swath Width	Spectral Bands	Spatial Resolution(m)	Application
1	Full	62	34	Aerosol
2	Full	18	17	Water
3	Full	18	17	Land
4	Full	18	17	Chlorophyll
5	Half	37	17	Land

1.3 BEAM toolbox development

Before we can exploit the advanced characteristics of CHRIS for scientific purposes, there are several pre-processing issues with the data that need to be resolved. These include noise reduction of striping in the across-track direction and pixels dropouts, geometric correction and image co-registration, cloud masking, and atmospheric correction of the top-of-atmosphere (TOA) radiances. In addition, spectral calibration of the smile effect is another complicating issue that needs to be considered. For CHRIS this can result in the narrow spectral bands being shifted by about 0.5 nm. Moreover, the spectral setting of each band can vary between acquisitions, owing to the thermal variations of the instrument and platform. As a result of these difficulties, the uptake of CHRIS data has been largely limited to experienced Earth observation scientists. Thus, ESA have procured a project for the development of a toolbox that allows the pre-processing of CHRIS data without recourse to the development of sophisticated in-house solutions. To achieve this goal both software developers and Scientists from around Europe are working closely together to implement these tools in a way that is straightforward to use. The aim is to incorporate all these modules into the BEAM (Basic Envisat AATSR and MERIS) open source software package that is freely available from www.brockmann-consult.de/beam under the Gnu Public License. In addition to

these pre-processing modules, a prototype module for aerosol optical depth (AOD) retrieval is also developed. Thus, users will be able to perform their own aerosol retrievals using a state-of-the-art algorithm.

1.4 Objectives

Our aim here is to develop an algorithm that exploits the multi-look and hyper-spectral capability of CHRIS for retrieving accurate estimates of aerosol properties. We will focus on the retrieval of AOD which is a key atmospheric parameter for both climate and air quality research. We present an algorithm that exploits the multi-view-angle capability of CHRIS for the retrieval of atmospheric aerosol optical depth (AOD) over land. Pre-calculated lookup tables of atmospheric properties for a given aerosol model allow computationally fast retrievals over entire CHRIS scenes.

The high spatial resolution of CHRIS will provide us with an unprecedented detail of atmospheric aerosols from space. This information will be useful for air quality mapping within towns and cities, for instance. For climate research its role will be important for inter-comparison with existing satellite aerosol products such as MODIS (MODerate resolution Imaging Spectrometer), MISR (Multi-angle Imaging Scanning Radiometer), (A)ATSR (Advanced Along Track Scanning Radiometer) and MERIS (Medium Resolution Scanning Radiometer), in addition to ground-based AERONET (Aerosol Robotic Network) sun-photometer observations (Holben *et al*., 1998). The fine spatial resolution will also allow us to examine the scaling effects of using ground-based point samples for validating relatively coarse (of the order of kilometers) satellite estimates of aerosol properties. An entire 13 by 13 km CHRIS scene approximately corresponds to a single pixel in many existing aerosol products (e.g. MODIS at 10 km and MISR at 17 km). Moreover, CHRIS with its multi-spectral and hyper-spectral capability will demonstrate what can be gained from improved sensor systems and allow us to identify optimal bands and viewing geometries for aerosol retrievals.

1.5 Document outline

The document is structured as follows. In Section 2 a brief discussion of atmospheric radiative transfer is given and description of the multi-view-angle AOD algorithm is presented. The processing scheme of the AOD retrieval module in outlined in Section 3. In section 4 testing is performed against a simulated

dataset of to-of-atmosphere (TOA) reflectances corresponding to the CHRIS instrument characteristics that are created from coupled surface and atmospheric radiative transfer model runs for a representative set of surface and atmospheric conditions. Validation at a range of sites worldwide against AERONET AOD is performed in Section 5. Finally we summarise the salient points in Section 6.

2 Description of AOD retrieval algorithm

2.1 Atmospheric radiative transfer

Satellite observations at optical wavelengths consist of solar radiation scattered by both the atmosphere and the surface. We need to separate out the atmospheric and surface scattering components through atmospheric radiative transfer modelling if we are to obtain accurate estimates of biophysical and geophysical properties. The atmospheric and surface contributions to the radiance measured by a spaceborne sensor at the top of the atmosphere for a given wavelength and viewing and illumination geometry over a Lambertian surface and for an absorbing atmosphere is given by the following atmospheric radiative transfer equation:

$$L_{toa} = L_0 + \frac{T(\theta_s) T(\theta_v) I_0 \rho_{surf}}{\pi [1 - \rho_{surf} S]} \, , \tag{1}$$

where L_0 is the atmospheric path radiance due to Rayleigh and aerosol scattering, ρ_{surf} is the surface reflectance, I_0 is the incident solar radiance at the top-of-the-atmosphere and is a function $\cos(\theta_v)$, S is the spherical albedo of the atmosphere, $T(\theta_v)$ is the transmittance from the surface to the top of the atmosphere in the view direction of the satellite, $T(\theta_s)$ is the transmittance from the top of the atmosphere to the surface along the path of the incoming solar radiation. All reflectance and radiances terms are a function of the the wavelength, solar θ_s and satellite θ_v zenith angles and relative azimuth angle, as well as the optical properties of the atmosphere and surface. The $1 - \rho_{surf} S$ term refers to multiple scattering between the surface and atmosphere but this term can be neglected for an optically thin atmosphere. We note that radiances can also be expressed as reflectance using:

$$\rho = \frac{\pi\, L}{I_0} \qquad\qquad\qquad (2)$$

The atmospheric path radiance L_0 can be separated into molecular L_M and aerosol L_A radiance scattering components such that

$$L_0 = L_M + L_A . \qquad\qquad\qquad (3)$$

The parameters required to model aerosol radiative effects are AOD τ , for a given reference wavelength, its spectral dependence, defined by Angstrom coefficient α, single scattering albedo ω and phase function $p(\Theta)$, where Θ denotes the scattering phase angle. These properties are closely related to aerosol mass loading, composition and size distribution. For aerosol retrieval we are particularly interested in the aerosol path radiance L_A. AOD is the principal property derived from satellite observations and is a function of the number and size of particles, integrated within an atmospheric column. The single scattering albedo is the ratio of scattered light to scattered and absorbed light. The phase function provides a description of the distribution of scattered radiation of the aerosol particles as a function of the scattering angle Θ . Climatologically defined aerosol models are used to constrain some of parameters (e.g. ω and p) in order for us to retrieve AOD.

To retrieve estimates of aerosol properties from measured satellite radiances, we need to solve the inverse problem and separate the atmospheric and surface scattering contributions to the observed signal. If the land surface is Lambertian then the differences between the measured radiances from the different viewing positions could be attributed to atmospheric path radiance only. However, all natural surfaces contain some degree of anisotropy at optical wavelengths, therefore it is necessary to consider how the bi-directional reflectance of the land surface changes with the viewing and illumination geometry in order to decouple the atmospheric and surface scattering contributions with any accuracy. For aerosol retrieval the difficulty lies in obtaining a reliable estimate of the land surface reflectance. Over bright land surfaces the problem is particularly challenging because surface scattering dominates the satellite signal. In addition, the land surface is heterogeneous and temporally varying making *a priori* assumptions difficult. Multi-view-angle observations such as those obtained from CHRIS have helped constrain the inverse problem since the surface is imaged through different atmospheric path lengths allowing us to infer the atmospheric properties and provide an angular constraint for the surface scattering that can be exploited

for the estimation of bi-directional reflectance.

Here, we present the algorithm that will be incorporated into the AOD module prototype. The algorithm exploits the multi-view-angle capability of CHRIS for AOD retrieval over land.

2.2 Multi-view-angle AOD retrieval algorithm over land

We need to obtain an accurate estimates of the surface reflectance if we are to obtain correspondingly accurate retrievals of the aerosol properties. The model of surface scattering presented here allows us to achieve this. In general, it is more challenging to retrieve aerosol properties over the land than the ocean. This is because the scattering from the land surface tends to dominate the satellite signal making it difficult to discern the atmospheric scattering contribution to the satellite signal particularly over bright surfaces. In addition, obtaining an accurate model of the land surface is further complicated because bi-directional reflectances are highly variable (North *et al.* 1999, Veefkind *et al.* 2000).

In contrast, atmospheric scattering dominates the signal over the ocean. PROBA/CHRIS was designed principally for land applications, but has found some applications over inland waters. Some algorithms algorithms, assume a negligible water leaving radiance in the near infrared region (Remer *et al.*, 2005). Atmospheric scattering dominates the signal over the ocean and at these wavelengths, we can infer that the measured satellite radiances is equal to the atmospheric path radiance. After correcting for gaseous absorption and Rayleigh scattering, the remaining contribution to the signal is atmospheric aerosol scattering. In reality, the presence of chlorophyll sediment and white caps can increase ocean reflectances so as to have non-zero water leaving radiances. As a result, for a given atmospheric profile, AOD can be overestimated as the unaccounted surface leaving radiance is integrated as part of the atmospheric path radiance to compensate. This is especially the case over inland waters where CHRIS images are acquired, and it is very difficult to retrieve AOD over these sites using these dark pixel approaches. More complex approaches using coupled ocean and surface lookup tables are required which is beyond the scope of implementation in the AOD retrieval module presented here, thus only AOD retiievals over water are performed.

A single-look AOD retrieval algorithm is used in the atmospheric correction of the CHRIS surface reflectances (Guanter *et al.,* 2007a, 2007b). This approach is based on the BAER algorithm of von

Hoyningen-Huene *et al*. (2003). The surface reflectance is calculated from a linear mixing model of *a priori* bare soil and vegetation spectra for all input spectral bands such that. The main disadvantage of this approach is that estimates of AOD are limited to dark vegetated surfaces and *a priori* estimates of the surface reflectance are required.

North *et al.* (1999) developed a simple physical model of light scattering for the dual-angle sampling of the ATSR-2 and AATSR instruments and can be used to separate the surface bi-directional reflectance from the atmospheric aerosol properties without recourse to *a priori* information of the land surface properties. This operational multi-look AOD retrieval approach is currently being implemented within ESA's GPOD (Grid Processing on Demand) environment for global retrievals of AOD from ATSR-2 and AATSR.   The core algorithm and science has been tested in North (2002) and Grey *et al.* (2006a, 2006b) and has not been extensively modified for implementation on CHRIS. Nonetheless, there has been some re-engineering to handle the different spectral and angular characteristics of CHRIS.

Previous studies have shown the shape of the surface bi-directional reflectance distribution function (BRDF) is similar at different wavelengths. This is because the scattering elements of the surface are much larger than light at optical wavelengths and so the angular variation of surface reflectance is dominated by wavelength independent geometric effects. This has been demonstrated by multi-angle observations from ATSR-2 and AATSR (*e.g.* Veefkind *et al*. 1998, 2000) and MISR (e.g. Diner e*t al*. 2005). For AATSR, the ratio of surface reflectances at the nadir (where the view zenith angle is close to 0°) and forward viewing angles (where the view zenith angle is 55°) is consistent between bands. Thus

$$\rho(\lambda_i, n) \approx \frac{\rho(\lambda_j, n)}{\rho(\lambda_j, f)} \rho(\lambda_i, f) \quad , \tag{4}$$

where nadir n and forward f refer to forward and nadir view zenith angles of (A)ATSR, respectively, and λ_i and λ_j are any combination of the (A)ATSR optical channels (550, 670, 870 1630 nm). At 1630 nm there is very little scattering and absorption owing to aerosols, thus correction for gaseous absorption and Rayleigh scattering will be sufficient for atmospheric correction. CHRIS does not have a shortwave infrared channel and even at the longest wavelength at around 1000 nm there is significant aerosol scattering.

North *et al.* (1999) developed this approach further by considering the variation of the diffuse fraction of light with wavelength, where scattering by atmospheric aerosols tends to be greater at shorter wavelengths. This is important to model because the fraction of diffuse to direct radiation influences the anisotropy of the surface. The anisotropy is reduced when the diffuse irradiance is high because the contrast between shadowed and sunlit surfaces decreases. Anisotropy is similarly dependent for bright targets owing to the multiple-scattering of light between the surface elements.   The atmospheric scattering elements including aerosols and gas molecules are comparable in size to the wavelength of light at optical wavelengths. As a result, the effect of atmospheric scattering on the anisotropy will be a function of wavelength and the shape of the BRDF will vary between channels. Considering these contributions results is a physical model of spectral change with view angle (North *et al.* 1999)

$$\rho_{mod}(\lambda, \Omega) = (1 - D(\lambda)) P(\Omega) w(\lambda) + \frac{\gamma w(\lambda)}{1-g}[D(\lambda) + g(1 - D(\lambda))] \quad , \tag{5}$$

where $g = 1 - \gamma w(\lambda)$, λ is the wavelength Ω is the viewing geometry (forward or nadir view in the cases of ATSR-2 and AATSR), ρ_{mod} is the modeled bidirectional reflectance, γ is the fraction contributing to higher-order scattering and is equal to 0.3 (North *et al.*, 1999), D is the fraction of diffuse irradiance, P is a wavelength independent parameter, and w is a parameter independent of the viewing and illumination geometry.

The first and second terms refer to direct and diffuse scattering, respectively.   The model separates the angular effects of the surface into two components, a structural parameter P that is dependent only on the view direction, and the spectral parameter, w , that is dependent only on the wavelength. $P(\Omega)$ and $w(\lambda)$ are the free parameters that we want to retrieve through model inversion.   If we assume that the influence of diffuse irradiance on surface reflectance is negligible then we get only the direct term which is analogous to (5) (Diner *et al.*, 2005)

$$\rho_{mod}(\lambda, \Omega) = P(\Omega) w(\lambda) \quad . \tag{6}$$

By inversion of (5), this model of surface scattering has been shown theoretically to lead to a tractable inversion method which is potentially more robust than the simple assumption of angular invariance alone (North *et al.*,1999). The angular reflectance of a wide variety of natural land surfaces have been

shown to fit this simple model (North *et al*.,1999). In contrast, reflectance that is a mixture of atmospheric and surface scattering does not fit this model well. As a result, the model can be used to estimate the degree of atmospheric contamination for a particular set of reflectance measurements and to find the atmospheric parameters which allow retrieval of a realistic surface reflectance. The minimum inputs into the algorithm are radiances from two bands and two solar and viewing geometries, so it can be applied to many existing multi-view-angle sensors.

2.3 Numerical inversion

Our aim is to retrieve AOD from multi-angle TOA cloud-free CHRIS radiances. This is achieved through a coupled inversion of the MODTRAN-4 radiative transfer model and the model of surface scattering. In practice, we use a set of pre-calculated lookup tables derived from MODTRAN-4 to allow for rapid inversions and to facilitate distribution with BEAM.

This inverse problem is under-constrained since it has fewer measurements than output model parameters that need to be retrieved. To regularise the problem so that AOD is the only unknown atmospheric parameter, assumptions must be made concerning the other aerosol optical properties including phase function and single-scattering albedo. In practice, a range of models representing generalised aerosol types are used to constrain the inverse problem. The atmospheric aerosol model is prescribed by the user from a choice of urban, continental, smoke, maritime and dust. The selection of model depends on the location and time of year and the accuracy of the AOD estimates will depend on how well the aerosol model characterises the actual atmospheric profile.

The inversion is achieved through iteration of a two stage numerical process (North *et al*.,1999), the schematic of which is presented in Figure 1. In this scheme the Powell multi-dimensional optimization routine is nested within the Brent one-dimensional numerical optimizer (Press *et al*.,1992). Neither optimisation routines require the partial derivatives of the equation's free-parameters. The first stage is to retrieve a set of surface reflectances and estimates of diffuse irradiance given an initial estimate of the atmospheric aerosol model and AOD at 550 nm by inversion of MODTRAN4. The best-fit of the two parameters P and w from (3) are found using Powell. The second stage uses Brent to converge on the optimum value for AOD. For each iteration, each estimate of AOD results in a different set of surface reflectance values. The optimum value of AOD is the best-fit of surface reflectances to the model (6), and

is attained by minimizing the error function E_{mod}

$$E_{mod} = \sum_{\Omega=1}^{5} \sum_{\lambda=1}^{62} \left[\rho_{surf}(\lambda, \Omega) - \rho_{mod}(\lambda, \Omega) \right]^2 \quad , \tag{7}$$

where ρ_{mod} is the surface reflectance estimated using (2) based on the best-fit values of the parameters P and w, and ρ_{surf} is the surface reflectance calculated using MODTRAN-4 given the TOA reflectance ρ_{toa} and the estimated atmospheric profile. Surface reflectance is related to the TOA reflectance by Vermote *et al.* (1997)

$$\rho_{surf}(\theta_s, \theta_v, \phi_s - \phi_v, \lambda) = \frac{\rho'_{TOA}}{1 + \rho'_{TOA} S} \quad , \tag{8}$$

where θ_s is the solar zenith angle, θ_v is the view zenith angle, ϕ_s is the solar azimuth angle, ϕ_v is the view azimuth angle, S is the atmospheric spherical albedo, and ρ'_{TOA} is

$$\rho'_{TOA} = \frac{\rho_{TOA}(\theta_s, \theta_v, \phi_s - \phi_v, \lambda) - \rho_{atm}(\theta_s, \theta_v, \phi_s - \phi_v, \lambda)}{T(\theta_s) T(\theta_v)} \quad , \tag{9}$$

where ρ'_{atm} is the intrinsic atmospheric reflectance, and $T(\theta_s)$ and $T(\theta_v)$ denotes downward and upward transmittance, respectively and is ρ_{toa} given by:

$$\rho_{toa} = \frac{\pi L_{toa}}{\cos(\theta_s) E_s} \quad , \tag{10}$$

where E_s is the solar radiance at the top of the atmosphere. AOD will be retrieved at 550 nm, but values of AOD can be attained at other wavelengths depending on the Angstrom coefficient of the selected aerosol model.
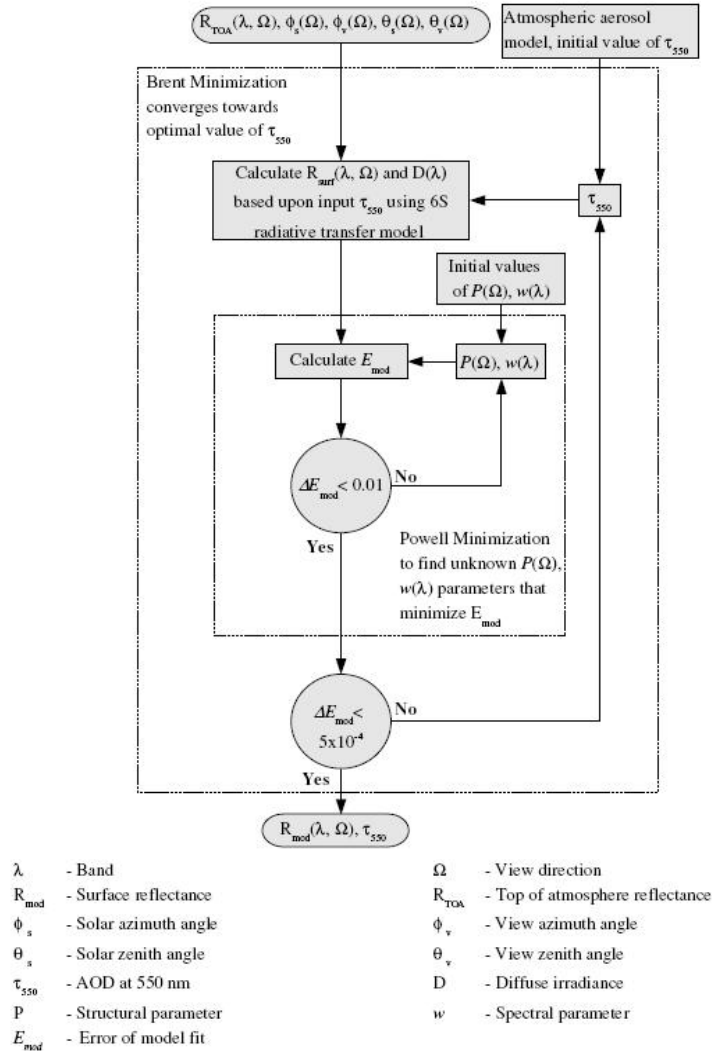
Figure 1: Schematic showing numerical inversion of AOD and surface reflectance retrieval (reproduced from Grey *et al*., 2006a).

2.6 Lookup tables

To achieve consistency with the atmospheric correction module we use the same MODTRAN lookup tables. This will allow us to directly use the retrieved value AOD in the atmospheric correction module. Pre-calculated lookup tables of atmospheric properties for a given aerosol model allow fast retrievals of AOD over entire CHRIS scenes of the order of a few minutes on a standard desktop computer. The lookup tables are created using the MODTRAN atmospheric radiative transfer model. The lookup tables

are constructed at 10 nm widths over the the the 400 – 1050 nm range of CHRIS. The dimensional parameters of the lookup tables are the SZA, VZA, RAA, elevation, water vapour and AOD (see Table 2). The values within the lookup tables are of the direct and diffuse radiance, fraction of diffuse-to-direct atmospheric transmittance, spherical albedo and path radiance (Guanter *et al.*, 2007b*)*. Currently there is one aerosol models based on a typical continental aerosol type, but other aerosol models can easily be generated and used in the AOD module. During operation, values are estimated in the lookup tables using multi-dimensional interpolation.

Table 2: Range of values of parameters and dimensions in the lookup tables (Guanter *et al.* 2007b).

Parameter	*Minimum value*	*Maximum value*	*No. of Steps*
AOD	0.05	0.6	6
Solar zenith angle	20°	64°	8
View zenith angle	0°	60°	8
Relative azimuth angle	0°	180°	7
Water vapour	0.3 g/cm^2	5 g/cm^2	7
Elevation	0 km	2.5 km	4

2.7 Band selection and spectral shift

We expect that the additional channels provided by CHRIS gives only a negligible improvement over using fewer channels in our retrievals of AOD. A complicating issue of hyper-spectral instruments is the need to account for the spectral shift of the bands because they are narrow, and a small shift can lead to a large difference in measured radiance as shown in Figure 2. Because we do not need all the CHRIS bands for the AOD retrieval we can ignore those wavelengths where the spectral shift is a significant problem.

We perform an experiment to identify the CHRIS bands that are less sensitive to the spectral shift. Figure 3 shows the effects of the spectral shift for the CHRIS bands at different modes. It is similar to the Green (1998) experiment but is limited to the CHRIS bands and a rectangular spectral response function with a 1 nm shift. In the strongly atmospheric absorbing regions at around 0.7 and 0.9 microns a small shift in the spectral calibration can lead to a big error in the measured radiance. Thus, relatively small lookup tables can be generated because we only use bands away from atmospheric absorption regions for aerosol

retrieval. This will help in two ways. Firstly, we do not need to consider water vapour as a dimension in the lookup tables and secondly, we do not need to worry about the spectral shift since we will be using channels away from the atmospheric absorption regions, in spectrally flat regions where a spectral offset will lead to only small errors, less than 1% of radiance according to Green (1998). With CHRIS there is approximately an offset of 0.5 nm. Channels that are likely to fall inside the strong absorption regions will not be considered in the AOD retrieval. We assume that there are no strong and narrow surface absorption features for AOD retrieval, as there at around 760 and 950 nm in the atmosphere.

Although we do not use the bands in the atmospheric absorption regions, we will still need to consider the changes in the spectral setting for each acquisition. These change because the spectral calibration is dependent on the instrument temperature and the band settings of each mode are different.
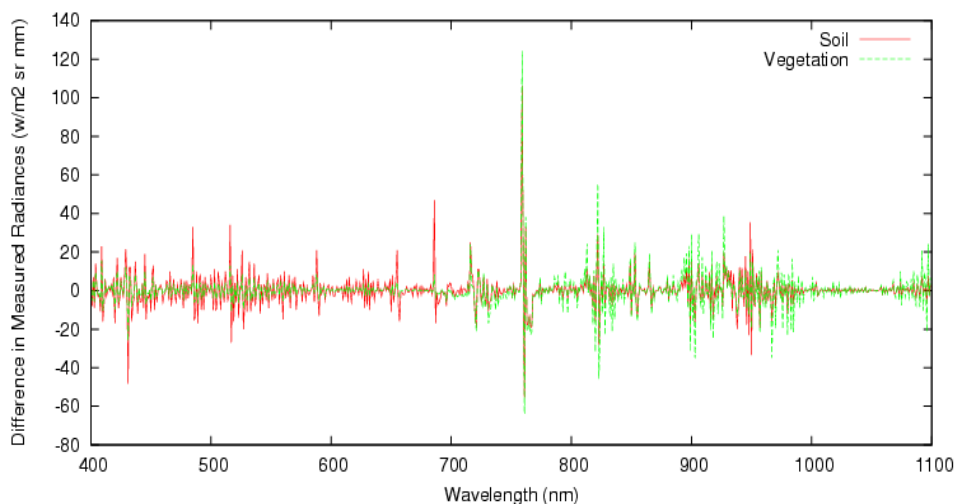

Figure 2: Difference in radiance due to spectral shift of 1nm. The radiance spectra are calculated for the TOA using MODTRAN-4 at a SZA of 30° and nadir view. The surface radiance spectra are for typical soil and vegetation. There is a large difference around 760 nm corresponding to a strong narrow oxygen absorption feature.
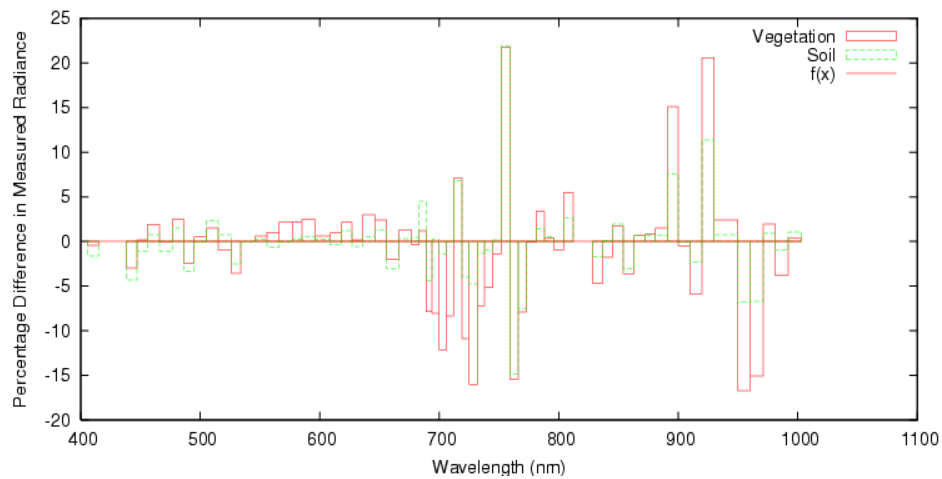
Figure 3: Percentage radiance error due to spectral shift of 1nm for CHRIS bands for Mode 1 following the experiments of Green (1998).   See Appendix for the other CHRIS modes.

3 Processing scheme of AOD retrieval

3.1 Pre-processing

The prerequisite for the AOD algorithms is a noise-free, cloud masked, and co-registered image set over land (see Figure 4). All the pre-processing steps can be performed within the BRAM CHRIS toolbox. Accurate estimates of aerosol properties are also required for atmospheric correction of the CHRIS top-of-the-atmosphere radiances. Within the processing scheme there is flexibility to use either the CHRIS retrieved estimates of AOD or an independent atmospheric profile such as from AERONET if estimates are available for the atmospheric correction. From surface reflectance it will then be possible to obtain quantitative biophysical properties such as albedo, LAI (leaf area index), and fAPAR (Fraction of absorbed photosynthetically active radiation) .

3.2 Processing Steps

We describe the processing steps for AOD retrieval from CHRIS. The steps include a set of tests that are performed prior to the model inversion including (1) cloud test, (2) water and land test, (3) heterogeneity test and (4) pixel aggregation. The user will have control over a number of these aspects of the AOD retrieval. These steps describe a pixel based AOD retrieval, but the algorithm is passed over the whole

CHRIS scene as illustrated in Figure 6. The AOD module ingests the pre-processed coregistered, cloud masked (but not atmospherically corrected) CHRIS radiances and outputs AOD at 550 nm. AOD at 440 and 660 nm are also calculated based on a parameterisation of the AOD at 550 nm and the Angstrom. The error of best fit is also output and gives an indication of the accuracy of the retrieval but it is difficult to interpret directly. A summary of statistics file is also output.

Selecting cloud free pixels - Owing to mis-registration between the different viewing geometries, CHRIS radiances are averaged within a small spatial window. This is a user-defined option with a default window size of 9 by 9 pixels. If there are no cloudy pixels within the window as identified by the cloud mask module, then we proceed to the next stage. Otherwise no aerosol retrieval is performed because there may by some undetected sub-pixel cloud contamination even within pixels flagged as cloud-free.

Selecting pixels over land or water - We need to identify whether our cloud-free pixel represent water or land surfaces, because the AOD algorithm can only be applied to land. Water surfaces are identified as such when the reflectances of all channels at wavelengths greater than 670 nm are less than 0.2, otherwise we consider the pixel to be land. Thus, if all of the pixels within the window are land then we can move onto the heterogeneity test, otherwise we do not perform the inversion for that pixel.

Heterogeneity test - A heterogeneity test for the pixels within the window is performed to improve the robustness of the retrieval. For instance, a boundary between two land covers within the window could cause problems for aerosol retrieval and so no retrieval is performed where the variance within the window is high. Otherwise, the radiances within the window are averaged and then the appropriate algorithm is applied to the dataset. The heterogeneity test is based on the standard deviation of radiances within the window for a given band.

3.3 Model inversion

The AOD module is flexible and can be applied to any CHRIS mode or band and angle combination. The flexibility on input configuration such as the number of input bands and looks is important because the 5 modes of CHRIS have different bands. In addition it is not always the case that 5 images are acquired for a site, but we should use as much of the angular information as is available because this will provide us with better estimates of AOD. Even for targets where five images were acquired, the overlap

with 5 looks will not occur over the entire nadir imaged scene (see Figure 6).   In most cases, approximately 60 percent of the nadir scene overlap with the other looks. For the multi-view-angle land AOD algorithm the minimum inputs are radiances from two bands and two solar and viewing geometries. The accuracy of the retrieved estimate of AOD depends on what data were ingested.   The more looks available the better our estimates of AOD.

Elevation information is required for very accurate retrievals of aerosol properties because information on surface pressure is needed for parameterising the Rayleigh scattering. High spatial resolution Digital Elevation Models are available at most CHRIS sites, but the IDL module does not use a DEM. It is relatively straightforward for the code to be modified to use a DEM though.
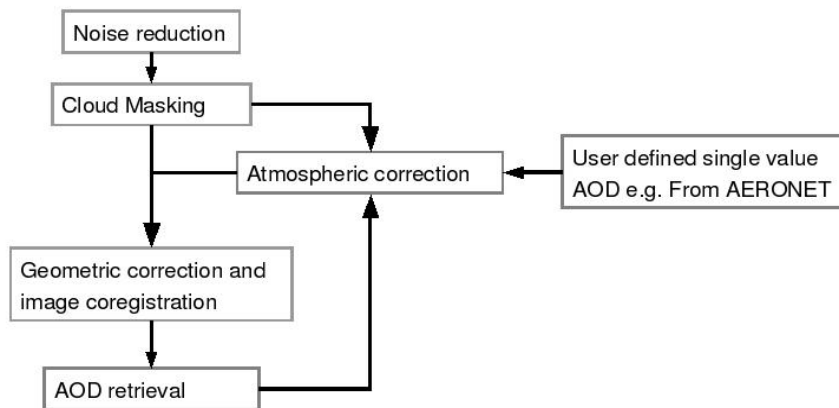
Figure 4: Processing flow for aerosol retrieval from CHRIS.

3.4 User Options and Limitations

There are a number of user options within the AOD module that makes it highly flexible.
- The application can be applied to any CHRIS mode or band and angle combination.
- The window size for pixel averaging can be specified and defines the spatial resolution of AOD retrievals across the scene.
- The algorithm is not limited to application over dark vegetated surfaces.

To keep the level of complexity to a minimum , there are inevitably some limitations of the AOD retrieval module.

- AOD is only retrieved at 550 nm although it is attaimned at other wavelengths based on the Angstrom for the aerosol model.

- Detailed information on aerosol properties including the particle size distribution are not retrieved. Instead these are prescribed in the aerosol models.

- Only one aerosol model is used, if the future more aerosol models can be generated and implemented.

- The elevation is fixed across the scene.

Despite these limitations the open-source philosophy of BEAM allows advanced users to modify the algorithms themselves and plug-in their own tools.
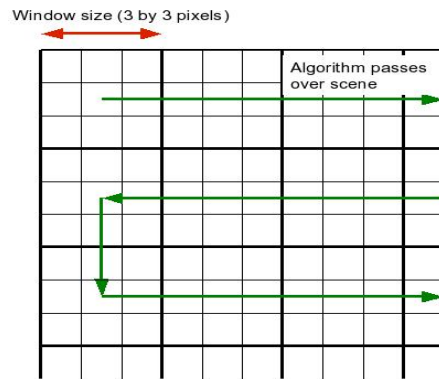

Figure 5: Algorithm pass over the CHRIS scene for an example 3 by 3 window.
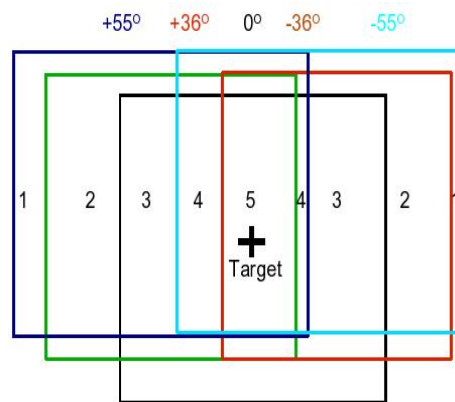

Figure 6: Schematic showing overlap of CHRIS images for a selected target.

4. Algorithm Testing

4.1 Generating the Simulated CHRIS dataset

The AOD retrieval algorithm is tested against a large set of simulated data that were created using coupled surface and atmospheric radiative transfer models for a range of atmospheric and surface conditions, corresponding to the CHRIS camera model and illumination geometries as shown in Table 3. For each land surface 8 different sets of reflectances are generated. The rationale for generating a representative dataset is to allow us to test the algorithm in a range of scenarios.

The Flight canopy radiative transfer model of North (1996) is used to generate a representative set of vegetated surfaces corresponding to forests and grasslands. A soil surface BRDF is produced using the Hapke soil model. The viewing and illumination conditions correspond to realistic PROBA/CHRIS geometries for the five looks. The channels used represent CHRIS data acquired under mode 3 but the algorithm can be applied to data acquired in any mode. The generated surface reflectances are then converted to TOA reflectances using the MODTRAN lookup table in the forward mode. We select a realistic atmospheric parameters for the corresponding land surface for a range of AODs. Finally Gaussian noise is added to the TOA reflectances in order to simulate poor calibration, image-registration and other potential sources of error. Figure 7 is a schematic illustrating how the models are coupled together to produce the simulated CHRIS TOA reflectance dataset.

4.2 Retrievals of AOD from the simulated dataset

We retrieve AOD at 550 nm from the generated TOA radiances by using the aerosol retrieval algorithm to solve the inverse problem.   The algorithms are applied to the simulated TOA reflectances. If the algorithms perform well then the retrieved AOD will be consistent with the AOD used in the forward model of the atmospheric radiative transfer to generate the TOA reflectances. Only four bands of CHRIS are used in the analysis corresponding approximately to the channels of the AATSR in the optical region (550, 670, 870 nm) except for the SWIR (shortwave infrared) channel where we use 910 nm channel as a replacement, because CHRIS does not have a SWIR channel. For the multi-angle retrievals all five look-angles are used. For the single-look retrievals over land only the nadir view retrievals are used. Inversions are performed on both the noise-free and Gaussian noise-added TOA reflectances. We use the

MODTRAN lookup table both in the forward and inverse modelling steps.

The RMSE of retrieved AOD at 550 nm, calculated by solving the inverse problem, against the AOD used in the forward model for generating the TOA reflectances is presented in Figure 8. Low RMSEs indicate that the algorithm is performing well. As expected for the noise-free dataset the retrievals of AOD are more accurate than the corresponding noisy dataset. The multi-view-angle method can retrieve AOD at 550 nm to within an RMSE of 0.03 for the simulated noise-free land surface.

Table 3: Characteristics of the simulated datasets.

| Atmospheric Parameters	
AOD at 550 nm	0.1, 0.4
Aerosol models	Continental
Camera model and illumination geometry	
Solar zenith angle	30°, 60°
View zenith angle	0°, 20°, 36°, 55°
Relative azimuth angle	0-180°
Channels (nm)	550, 670, 870, 910
Surface parameters	
Soil	Hapke Model, Dark soil spectra, Desertic and Continental aerosol models
Vegetation	Prospect veg spectra, dark soil spectra, FLIGHT, Continental and biomass aerosol models
Dense forest	LAI=4.0, fCover=0.9, fraction of senescent veg spectra=0.0
Sparse forest	LAI=2.0, fCover=0.2, fraction of senescent veg spectra=0.15
Green vegetation	LAI=2.0, fCover=1.0, fraction of senescent veg spectra=0.0
Senescent vegetation	LAI=2.0, fCover=1.0, fraction of senescent veg spectra=1.0
Sparse vegetation	LAI=0.5, fCover=1.0, fraction of senescent veg spectra=0.0
Noise	None, Gaussian noise with standard deviation of 0.05, 0.1, 0.2
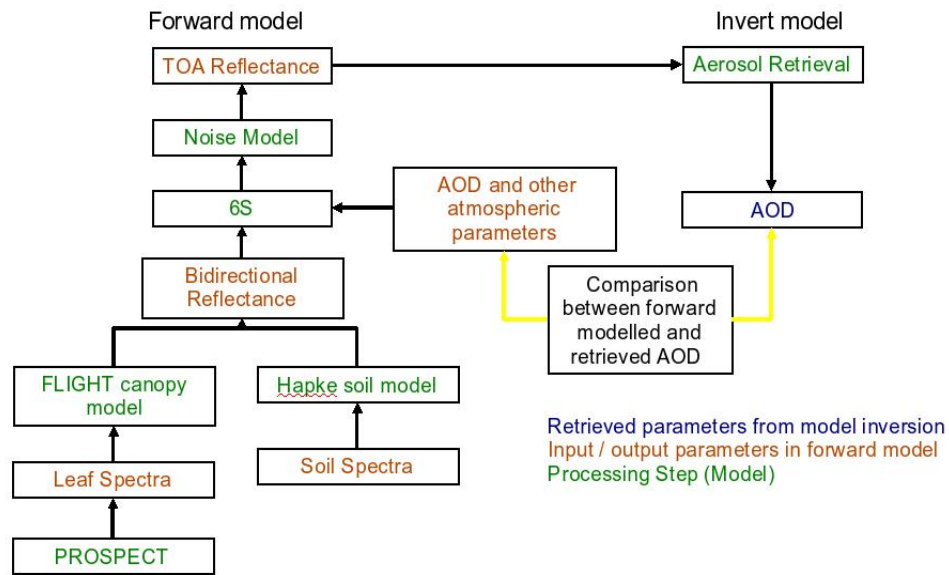
Figure 7: Schematic illustrating how the models are coupled together to produce the simulated CHRIS TOA reflectance dataset. The retrieved AOD values are compared with those used in the forward modelling.
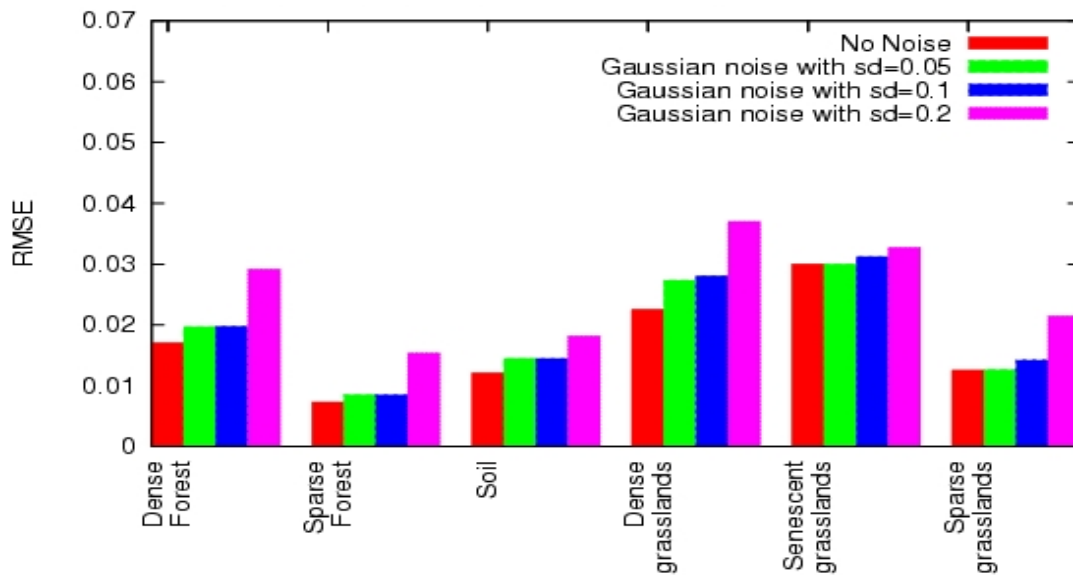

Figure 8: RMSE of CHRIS AOD retrievals using the multi-view-angle approach against forward modeled AOD at 550 nm.

5. Validation against AERONET

5.1 Image selection and pre-processing

While it is useful using simulated data in order to evaluate the AOD algorithm, we also need to perform validation of the PROBA/CHRIS retrievals of AOD against AERONET observations. Validation of CHRIS data against ground-based AERONET sun-photometers is difficult because there is not a large representative set of sites worldwide where there are coincident observations of the two instruments. Nevertheless testing has been performed for 29 relatively cloud-free scenes at six AERONET sites around the world at which sun-photometer observations are coincident with the satellite overpass. These sites also correspond to a range of land covers including urban, arid, agriculture and mixed vegetation (see Table 3). This represents a robust test for the algorithm because the urban and agricultural scenes are heterogeneous and the desert targets with their bright surfaces mean that surface scattering dominates and the atmospheric scattering only represents a small portion of the signal. Each CHRIS scene covers an area of about 13 by 13 km. Only CHRIS mode 1 scenes with a spatial resolution of 34 m at nadir were processed, but the algorithm can be applied to any CHRIS mode.

Table 3: AERONET sites used for validation of the PROBA/CHRIS AOD retrievals.

Site	Surface	Lat	Lon	Number of scenes
Chilbolton, UK	Agricultural	51.14	-1.44	1
Cart Site, Great Plains, US	Agricultural	36.60	-97.49	4
Lake Argyle, Australia	Mixed vegetation	-16.10	128.77	5
Mexico City, Mexico	Urban	19.33	-99.18	4
Solar Village, Saudi Arabia	Arid	24.90	46.40	8
Tinga Tingana, Australia	Arid	-28.98	139.99	7

Prior to performing the model inversions for AOD retrieval, noise removal routines have been applied to the CHRIS data in order to reduce the influence of vertical striping and to remove pixel dropouts. In addition, a cloud mask has also been applied to the only cloud scene at Chilbolton.

The AOD retrieval tool is very flexible and allows us to use any combination of viewing angles and bands and CHRIS modes. While CHRIS has five looks only two looks were used (nadir and plus 55 / minus 55 look angles) in the inversions for AOD retrieval. This is because the collocation between the

scenes needs to be performed using between 10 and 30 manually selected ground control points. This is a very time consuming task, but an automated method of geo-location is currently under development at the University of Valencia. The off-nadir scenes are warped to the nadir base image using a polynomial with nearest-neighbour interpolation. Whether the plus 55 or minus 55 looks were used depended on the scattering angle. Previous work has shown that accuracy in AOD retrieval with a large scattering angle leads to less accurate results that with a small scattering angle because aerosols tend to be forward scattering. Thus we select combinations where the scattering angle of the off-nadir view is small.

Only four bands in the non-absorbing region were used in the retrieval. These were bands 13, 24, 52 and 62 of mode 1 corresponding to wavelengths of around 550 nm, 665 nm, 890 nm and 1000 nm although the exact wavelength varies between PROBA/CHRIS acquisitions. Inversions were performed over 9 by 9 windows across the scenes, thus covering an area of approximately 300 metres square.

The inversion generally takes about 4-5 minutes processing time (using 2 looks and four bands in Mode 1 and 340 m resolution). The inversion was performed across all 29 scenes. As well as AOD at 550 nm, we also output AOD at 440 nm and 660 nm based on a simple parameterisation of Angstrom of the aerosol model. An error image of best fit of the model for each inversion and a file of summary of statistics for the images are also output automatically. A true colour composite nadir image of Solar Village acquired on 18/03/2003 and the corresponding map of CHRIS derived AOD over the scene is shown in Figure 9. The dimensions of the images is approximately 13 by 13 km. The average AOD across the CHRIS scene is 0.16 and at the AERONET site it is 0.22. The CHRIS derived AOD is relatively constant across the scene. Areas in black indicate locations where no retrievals are made principally due to the large variance of radiances within the 9 by 9 window.

5.2 CHRIS and AERONET comparison

The mean AOD across each image is calculated and compared with the AERONET as shown in Figure 10. The error bars indicating the standard deviation of the AOD across the scene. Across all sites the Pearson's correlation coefficient has been calculated to be 0.69 (p<0.0001) with a RMSE (root mean square error) of 0.11.

At Tinga Tingana AOD is less than 0.1 at 550 nm for all scenes. The residual differences between the

PROBA/CHRIS and AERONET derived estimates of AOD are small for this site. However, the variability of AOD between scenes is small compared with the error in the retrieved AODs. There is a large variability of AOD across Mexico City which is a good demonstration of CHRIS capability because previously researchers assume that AOD is constant at kilometer scales. MODIS and MISR retrieve at 10km and 17km respectively, but we have shown for the first time from space that AOD varies at the scale of the order of hundreds of meters. However the small scale variability across the scene makes direct comparison with AERONET difficult as this is only acquired at a single point in the scene.

Lake Argyle shows the least impressive results of all sites and AATSR also has difficulty retrieving over this site. However, preliminary investigations selecting pixels on the basis of high NDVI have shown improvements at this site. At the Cart Site on the Great Plains there is also small variability of AOD between different dates on which the image data were acquired. Agreement between CHRIS and AERONET derived AOD at Solar Village is good although the satellite retrievals do underestimate AOD at high concentrations. This may be partly due to the use of an aerosol model that does not properly characterise the atmospheric profile. At all sites uncertainties in calibration and coregistration error may lead to less accurate retrievals of AOD.
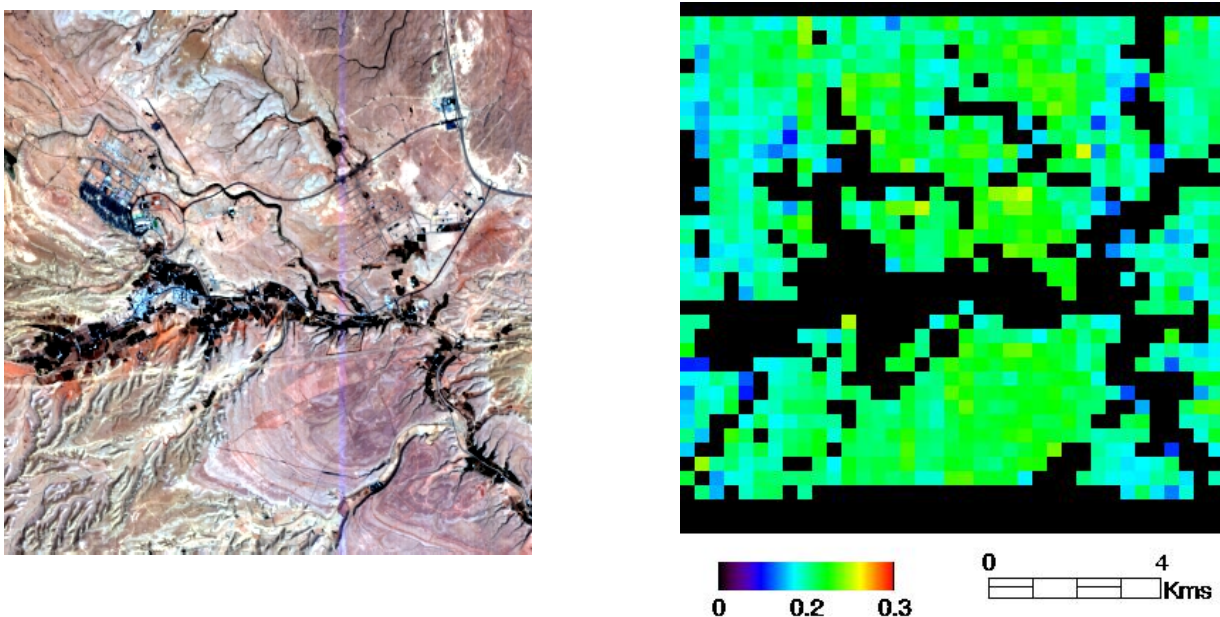

Figure 9: True colour composite nadir image of Solar Village acquired on 18/03/2003 and the corresponding map of CHRIS derived AOD over the scene. The dimensions of the images is approximately 13 by 13 km. The average AOD across the CHRIS scene is 0.16 and for AERONET it is 0.22. © SSTL.
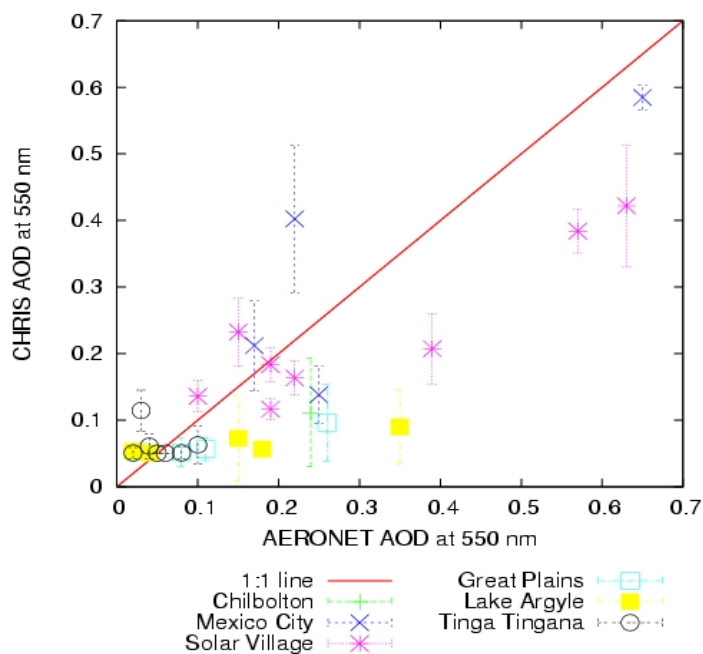
Figure 10: PROBA/CHRIS versus AERONET AOD at 550 nm at six sites worldwide. Pearson's r^2 is 0.69 (p<0.0001), the number of samples is 29, and the RMSE is 0.11.

6. Summary

We have developed an AOD retrieval module that will be made freely available through BEAM. It will allow users to perform their own AOD retrievals of CHRIS data using a state-of-the-art multi-view-angle AOD algorithm. Testing of the algorithm based on a simulated dataset shows good agreement. The multi-view-angle land AOD retrieval method has also been tested for CHRIS data at six AERONET sites worldwide. Across all sites the Pearson's correlation coefficient has been calculated to be 0.69 with a RMSE (root mean square error) of 0.11.

The prototype itself is written in IDL and is completely flexible for the number of looks, channels and CHRIS modes. The code is controlled by an input card that the user edits and specifies a number of parameters and datasets to read in. It operates over whole CHRIS scenes and the user also has control over the resolution at which the AOD retrievals can be performed. To retrieve AOD over a CHRIS scene takes about 4-5 minutes processing time (using 2 looks and four bands in Mode 1 and 340 m resolution). As well as AOD at 550 nm, we also output AOD at 440 nm and 660 nm based on a simple

parameterisation of Angstrom of the aerosol model. An error image of best fit of the model for each inversion and a file of summary of statistics for the images are also output automatically.

The main limitation of the algorithm is that retrievals cannot be performed over water. Also where a single-look image is not available aerosol inversions cannot be performed. Only one aerosol model is used currently corresponding to generic continental conditions, however more lookup tables with different aerosol models can be easily generated in any future developments of the module.

The potential implementation of the AOD algorithm in Java can be relatively straightforward. Some of the routines are consistent with those used for atmospheric correction (e.g. lookup table reading and interpolation and numerical routines), other routines are generic I/O routines, which are already implemented in BEAM. The novel aspects of the code (i.e. these are the core sceintific algorithms) have been written in Java already. By piecing these elements together it can be a relatively straightforward to put the AOD retrieval algorithm into BEAM in the future.

The unique characteristics of CHRIS will mean that this instrument will have an important contribution to play in understanding atmospheric aerosols over small areas. The retrieved AOD can also be used in the atmospheric correction module, because the lookup tables used will be the same. The high-level specification of CHRIS will also allow extensive experimentation. The flexibility of the inversion allows experimentation with a variety of combinations of modes, resolutions, bands and viewing angles. This will help us to find an optimal combination and possibly influence the design and development of future satellite missions and algorithms for aerosol research.

Acknowledgments

References

Barnsley, M., Settle, J., Cutter, M., Lobb, D., and Teston, F. The PROBA/CHRIS mission: a low-cost smallsat for hyperspectral, multi-angle, observations of the Earth surface and atmosphere. *IEEE Trans. Geosci. Remote Sensing*, 42(7), 1512-1520, 2004.

Green, R.O., 1998, Spectral calibration requirement for Earth-looking imaging spectrometers in the solar-reflected spectrum, *Applied Optics*, 37 (4), 683-690.

Grey, W., P. North., and S. Los, Computationally efficient method for retrieving aerosol optical depth from ATSR-2 and AATSR data, *Applied Optics*, vol. 45, no. 12: pp. 2786-2795, 2006.

Grey, W., P. North., S. Los, and R. Mitchell, Aerosol optical depth and land surface reflectance from multi-angle AATSR measurements: Global validation and inter-sensor comparisons, *IEEE Trans. Geosci. Remote Sensing* , vol. 44, no. 8, pp. 2184--219, 2006

Guanter, L., M. Del Carmen Gonzalez-Sanpedro, and J. Moreno, A method for the atmospheric correction of ENVISAT/MERIS data over land targets, *International Journal of Remote Sensing*, 28,3-4, 709-728, 2007a.

Guanter, L., L. Alonso, L. Gomez-Chova, and J. Moreno, CHRIS/PROBA Atmospheric Correction Module ATBD, CHRIS toolbox, 2007b.

North, P. Three-dimensional forest light interaction model using a Monte Carlo method, *IEEE Trans. Geosci. Remote Sensing*, 34(4), 1996.

North, P., S. Briggs, S. Plummer, and J. Settle, Retrieval of land surface bidirectional reflectance and aerosol opacity from ATSR-2 multi-angle imagery, *IEEE Trans. Geosci. Remote Sensing*, 37(1), 526-537, 1999.

North, P., 2002, Estimation of aerosol opacity and land surface bidirectional reflectance from ATSR-2 dual-angle imagery: operational method and validation, *Journal of Geophysical Research*, 107(D12) 7, no. 4149, 2002.

Press, W., S. Teukolsky, W. Vetterling, and B. Flannery, *Numerical Recipes in C*, Cambridge University Press, Second Edition, pp 994, 1992.

Vermote, E., D. Tanre, J. Deuze, M. Herman, and J.-J. Morcette, Second simulation of the satellite signal in the solar spectrum, 6S: An overview, *IEEE Trans. Geosci. Remote Sensing*, 35(3), 675-686, 1997.

Diner, D., J. Martonchik, R. Kahn, B. Pinty, N. Gobron, D. Nelson, and B. Holben, Using angular and spectral shape similarity constraints to improve MISR aerosol and surface retrievals over land, *Remote Sensing of Environment*, vol. 94, pp. 155--171, 2005.

Holben, B., Y. Kaufman, T. Eck, I. Slutsker, and D. Tanre, AERONET - A federated instrument network and data archive for aerosol characterization, *Remote Sensing of Environment*, 66, 1-16, 1998.

Remer, L.A., Y. J. Kaufman, D. Tanre, S. Mattoo, D. A. Chu, J. V. Martins, R.-R. Li, C. Ichoku, R. C. Levy, R. Kleidman, T. F. Eck, E. Vermote, and B. N. Holben, The MODIS Aerosol Algorithm, Products and Validation, *Journal of the Atmospheric Sciences*, vol. 62, pp. 947--973, 2005.

Sira, Chris data format, Doc. 271.DO.13, Issue 4.2, 2005.

Veefkind, J.P., G. de Leeuw, and P.A. Durkee (1998), Retrieval of aerosol optical depth over land using two-angle view satellite radiometry during TARFOX, *Geophysical Research Letters*, 25 (16), 3135-3138, 1998.

Veefkind, J.P., G. de Leeuw, P. Stammes, and R.B.A. Koelemeijer (2000), Regional distribution of aerosol over land, derived from ATSR-2 and GOME, *Remote Sensing of Environment*, 74, 577-386.

von Hoyningen-Huene, W., M. Freitag, and J. B. Burrows, Retrieval of aerosol optical thickness over land surfaces from top-of-atmosphere radiance, *J. Geophys. Res.,* 108(D9), 4260, doi:10.1029/2001JD002018, 2003.

Appendix

Annex 1 - Nominal CHRIS bands for modes 1-5.

Mode 1

Band	λ (nm)	Band	λ (nm)	Band	λ (nm)	Band	λ (nm)	Band	λ (nm)	Band	λ (nm)	Band	λ (nm)
1	411	10	520	19	**613**	28	691	37	**748**	46	833	55	915
2	442	11	530	20	622	29	697	38	755	47	841	56	925
3	452	12	**540**	21	**631**	30	703	39	762	48	850	57	940
4	461	13	**551**	22	641	31	709	40	770	49	859	58	955
5	**471**	14	561	23	651	32	716	41	**777**	50	**868**	59	965
6	481	15	572	24	661	33	722	42	785	51	877	60	976
7	490	16	581	25	**672**	34	728	43	792	52	**886**	61	987
8	**500**	17	590	26	**680**	35	735	44	**800**	53	895	62	**997**
9	**510**	18	**603**	27	686	36	742	45	808	54	905		

Mode 2

Band	λ (nm)	Band	λ (nm)
1	411	10	651
2	442	11	**672**
3	490	12	**680**
4	**510**	13	686
5	530	14	706
6	561	15	755
7	570	16	**781**
8	590	17	**872**
9	622	18	**1019**

Mode 3

Band	λ (nm)	Band	λ (nm)
1	442	10	703
2	490	11	709
3	530	12	742
4	**551**	13	**748**
5	570	14	**781**
6	**631**	15	**872**
7	661	16	895
8	**672**	17	905
9	697	18	**1019**

Mode 4

Band	λ (nm)	Band	λ (nm)
1	489	10	709
2	**551**	11	716
3	**631**	12	735
4	**672**	13	742
5	**680**	14	**748**
6	686	15	755
7	691	16	**777**
8	697	17	785
9	703	18	792

Mode 5

| Band	λ (nm)	Band	λ (nm)	Band	λ (nm)	Band	λ (nm)	Band	λ (nm)
1	442	10	697	19	755	28	905	37	**1019**
2	489	11	703	20	762	29	915		
3	530	12	709	21	770	30	925		
4	**551**	13	716	22	**777**	31	940		
5	570	14	722	23	792	32	955		
6	**631**	15	728	24	**800**	33	965		
7	661	16	735	25	**872**	34	976		
8	**672**	17	742	26	**886**	35	987		
9	683	18	**748**	27	895	36	**997**		

Only the highlighted channels are used in the AOD retrieval scheme and correspond approximately to the bands in Annex 2.

## Annex 2 - CHRIS bands selected for AOD for modes 1-5.

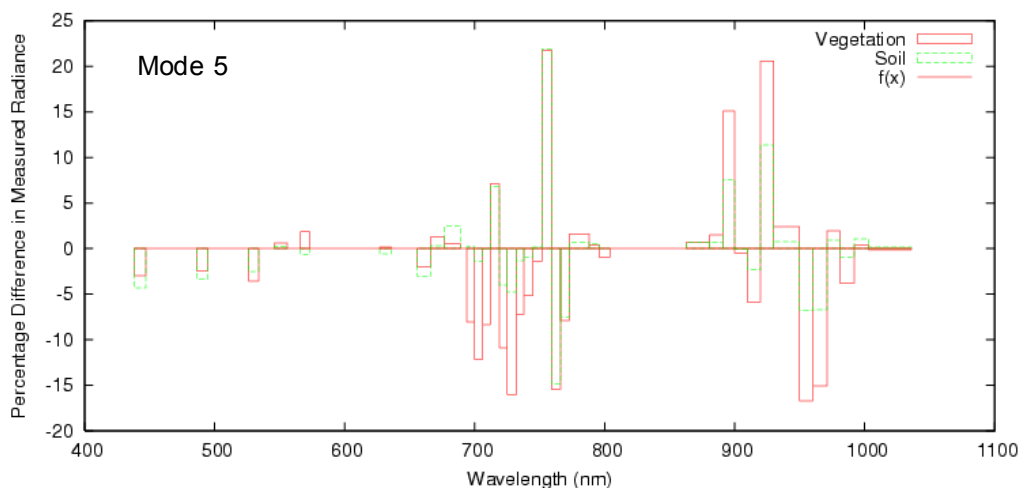| Band	Mode 1	Mode 2	Mode 3	Mode 4	Mode 5
510	9	4	-	-	-
540	12	-	-	-	-
551	13	-	4	2	4
603	18	-	-	-	-
613	19	-	-	-	-
631	21	-	6	3	6
672	25	11	8	4	8
680	26	12	-	5	-
748	37	-	13	14	18
777	41	-	-	16	22
781	-	16	14	-	-
800	44	-	-	-	24
868	50	-	-	-	-
872	-	17	15	-	25
877	51	-	-	-	-
886	52	-	-	-	26
997	62	-	-	-	36
1019	-	18	18	-	37

Annex 3 - Nominal CHRIS bands for modes 1-5 with spectra.
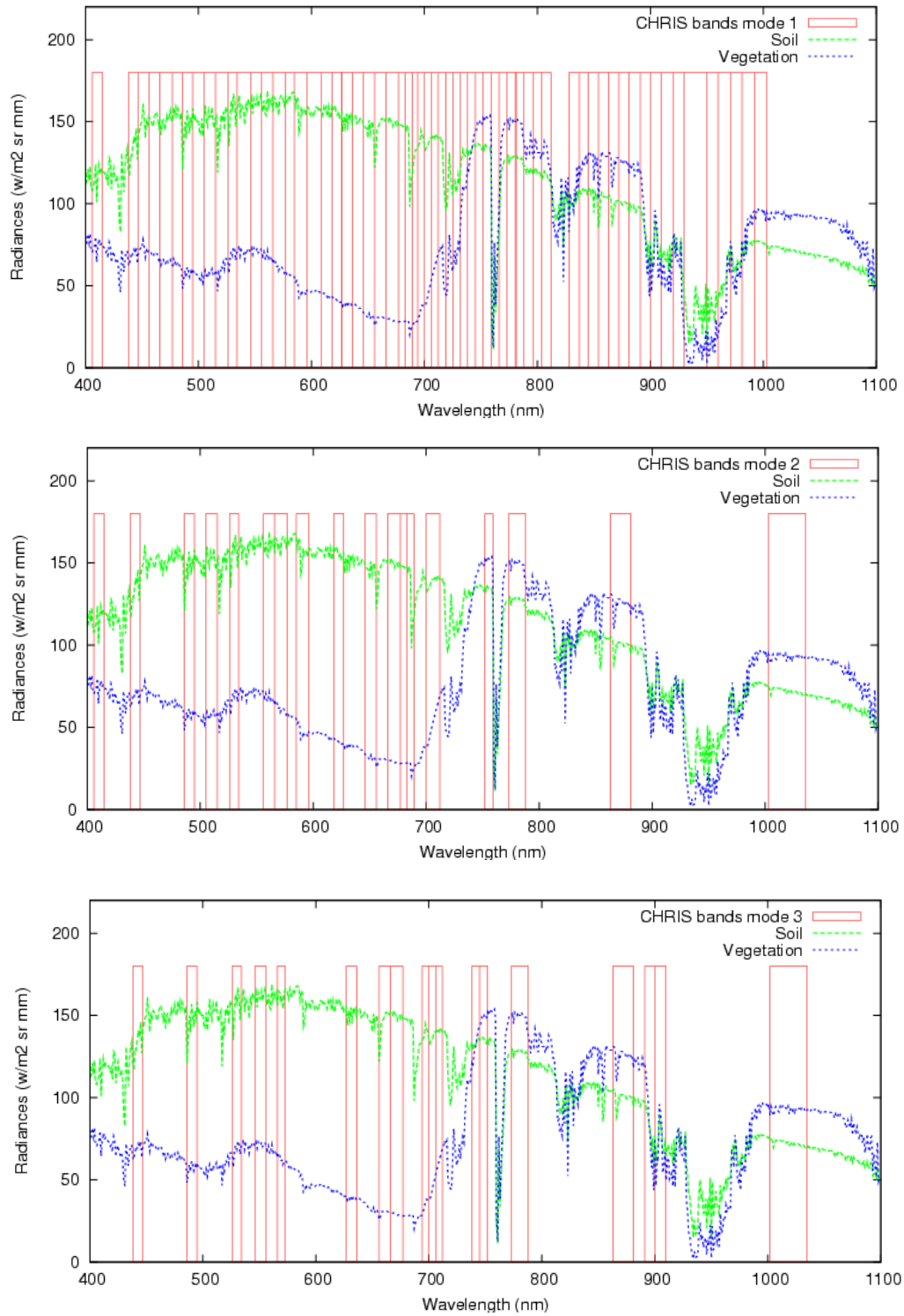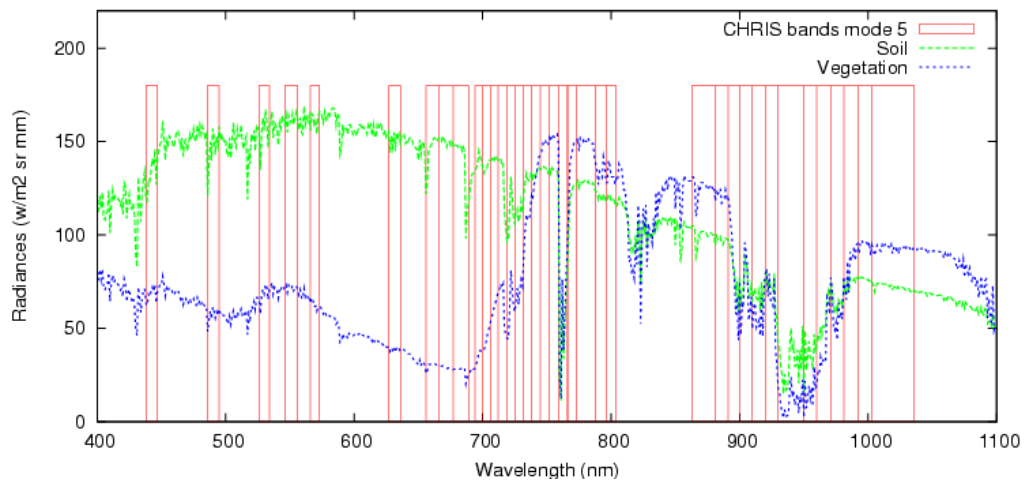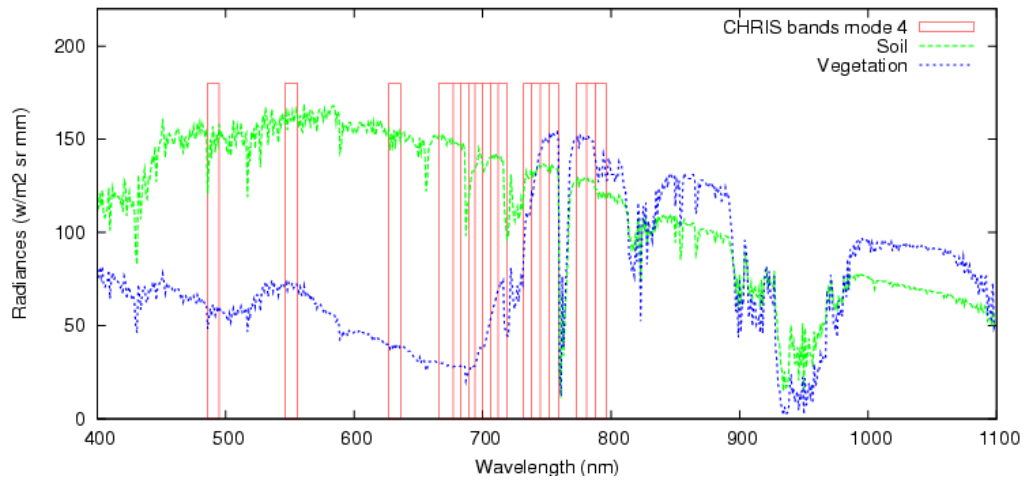
Annex 4 - Percentage radiance error due to spectral shift of 1nm for CHRIS bands Modes 2-5.
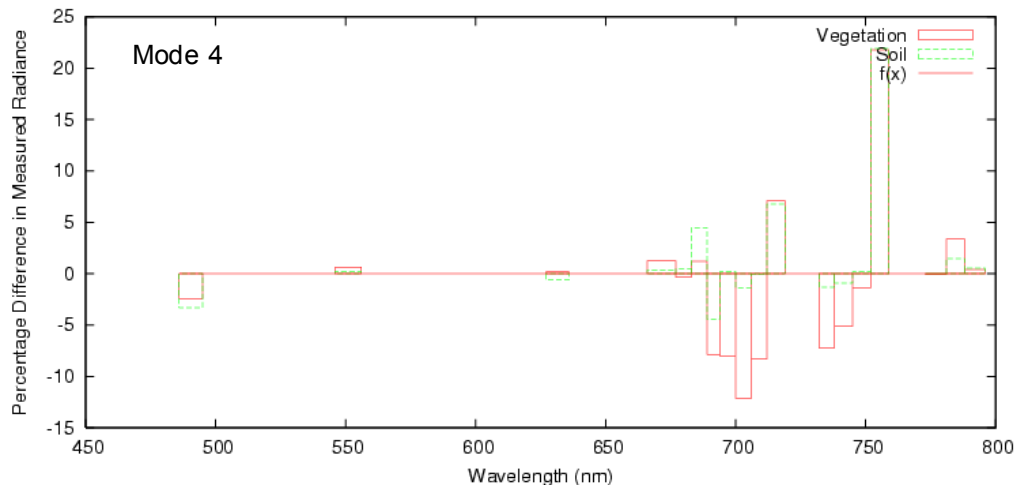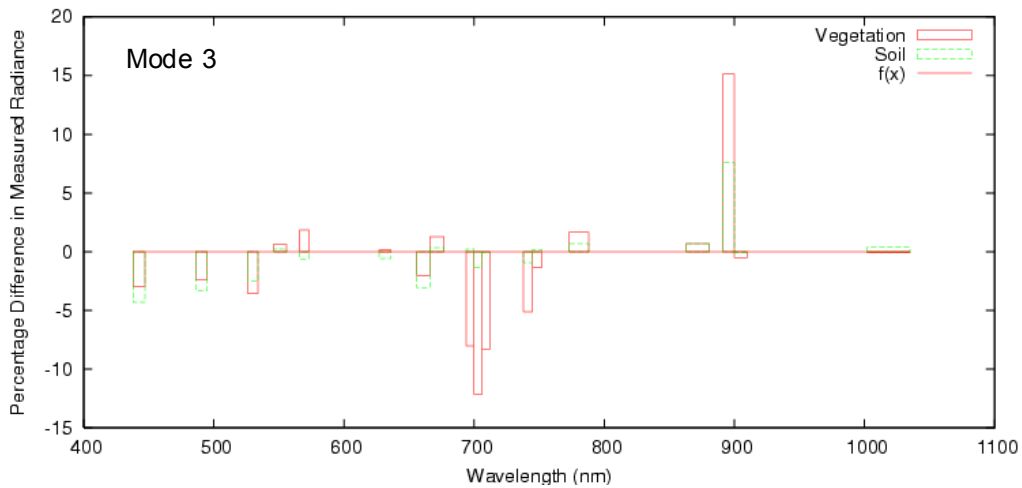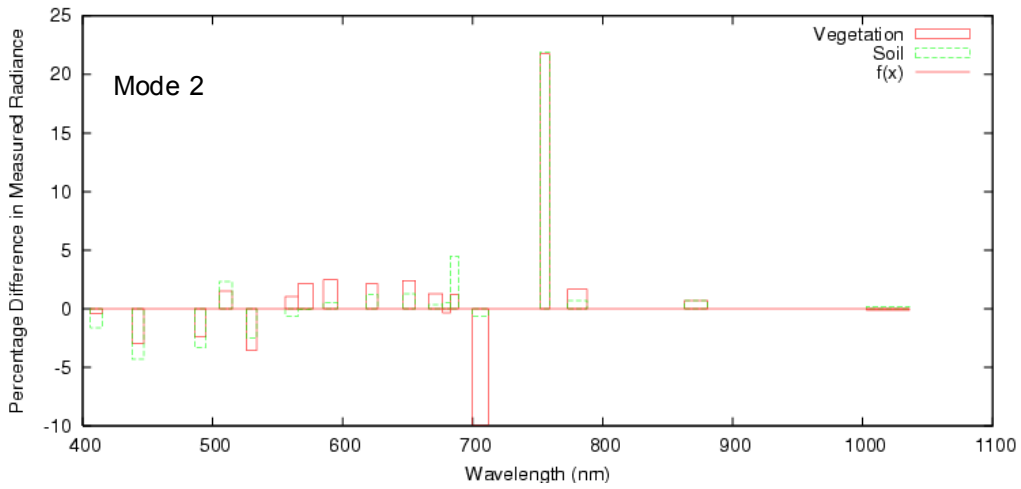
Annex 5 – AOD module operation in IDL.

To run type the following at the IDL command prompt:

chris_pt_aod_lut_img, 'input_card.dat'

Example input card

```
chris_merged.data [inputfile]        # CHRIS merged image DIMAP directory
CHRIS_LUT_formatted_1nm              # Lookup table of atmospheric parameters
372 374                              # Pixels Lines
5                                    # Select number of looks
51.0 125.1 19.19 316.00 Nadir        # SZA, SAZ, VZA, VAZ,  view 1
51.0 125.1 38.69 345.50 Plus35       # SZA, SAZ, VZA, VAZ,  view 2
51.0 125.1 36.88 212.23 Minus35      # SZA, SAZ, VZA, VAZ,  view 3
51.0 125.1 57.18 357.35 Plus55       # SZA, SAZ, VZA, VAZ,  view 4
51.0 125.1 55.71 203.37 Munus55      # SZA, SAZ, VZA, VAZ,  view 5
4                                    # Number of channels
0.549 0.05 b3                        # WlMid, WlWidth, band number 1
0.671 0.11 b13                       # WlMid, WlWidth, band number 2
0.868 0.09 b25                       # WlMid, WlWidth, band number 3
0.987 0.11 b50                       # WlMid, WlWidth, band number 4
1                                    # CHRIS Mode (1,2,3,4 or 5)
6 0.1                                # Aerosol model, angstrom
2.5                                  # Column water vapour (g/cm²)
0.35                                 #Ozone (DU/1000)
0.0                                  # Elevation (m)
9                                    # Window size
10                                   # Skip
```

Example input DIMAP files

```
radiance_b13Minus35.img   radiance_b13Plus35.img  radiance_b13Nadir.img
radiance_b24Minus35.img   radiance_b24Plus35.img  radiance_b24Nadir.img
radiance_b52Minus35.img   radiance_b52Plus35.img  radiance_b52Nadir.img
radiance_b62Minus35.img   radiance_b62Plus35.img  radiance_b62Nadir.img

radiance_b13Minus55.img  radiance_b13Plus55.img
radiance_b24Minus55.img  radiance_b24Plus55.img
radiance_b52Minus55.img  radiance_b52Plus55.img
radiance_b62Minus55.img  radiance_b62Plus55.img
```

Output files

aot550.img	*Raw binary image of retrieved AOD at 550 nm (size is rows by columns by float)*
aot550_err.img	*Corresponding error image of model best-fit*
aot440.img	*AOD at 440 nm parameterised from AOD at 550 nm and Angstrom*
aot670.img	*AOD at 440 nm parameterised from AOD at 550 nm and Angstrom*
aot_stats.dat	*Ascii text file of summary of statistics of AOD*